2.2 Fracture Mechanics Fundamentals

Fracture Mechanics is that technology concerned with the modeling of cracking phenomena. Bulk (smooth specimen) properties are not normally useful in design for determining a material's tolerance to cracks or crack-like defects, because material tolerance to flaws resides in a material's ability to deform locally. Since the source of fractures can be identified with the lack of material tolerance to cracks, it seems only natural that attention should be focused on the crack tip region where the material must resist crack extension. This section will introduce the principal features of a mechanical model that characterizes a crack movement in structural components fabricated from materials having low tolerance to flaws.

Some basic information that a designer should be familiar with prior to the utilization of remaining sections of this handbook is presented. This subsection will define the meaning and use of the fracture mechanics model for the control of fracture and sub-critical crack growth processes.

The application of a fracture mechanics model to solve crack problems came about through the following realization: component fractures that result from the extension of small crack-like defects are failures that depend on localized phenomena. Consider the three independent modes of crack extension that are illustrated in Figure 2.2.1. The tensile opening mode, Mode 1, represents the principal action observed and this is the type of separation that we design against. While fractures induced by shear stresses can occur, these fractures are rather infrequent. There are hypotheses available for describing the combined influence of two (or three) modes of crack extension but these will not be discussed until Section 4. In general, since improvement of a material's Mode 1 fracture resistance will also improve the resistance to the combined mode action, the development of concepts throughout the Handbook will emphasize Mode 1 crack extension behavior.

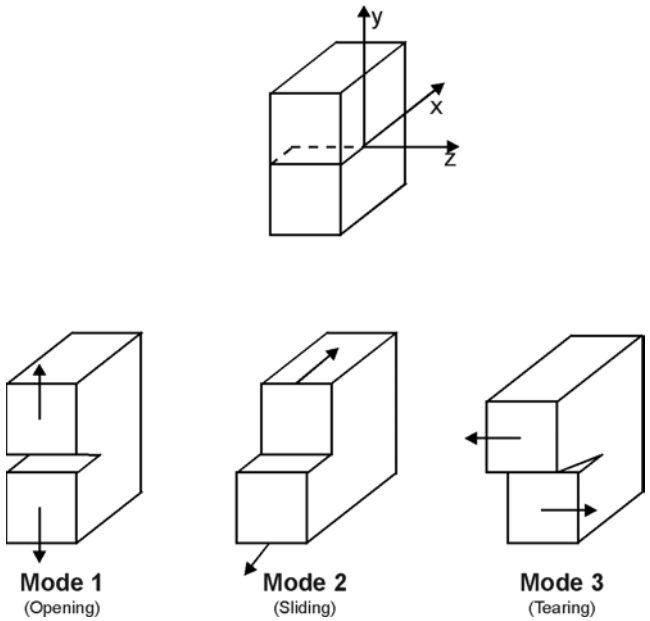

Figure 2.2.1. The Three Modes of Crack Extension

A linear elastic analysis of a cracked body provides a good first approximation to the localized stress state in materials that fracture at gross section stresses below the yield strength. No additional refinements in the analysis are necessary if the gross section stresses at failure are below $0.7\sigma_{ys}$. The elastic analysis when modified to account for restricted amounts of stress relaxation due to crack tip plastic deformation provides an adequate description of fracture that occurs above $0.7\sigma_{ys}$.

2.2.1 Stress Intensity Factor – What It Is

The model referred to above is called the linear elastic fracture mechanics model and has found wide acceptance as a method for determining the resistance of a material to below-yield strength fractures. The model is based on the use of linear elastic stress analysis; therefore, in using the model one implicitly assumes that at the initiation of fracture any localized plastic deformation is small and considered within the surrounding elastic stress field. Application of linear elastic stress analysis tools to cracks of the type shown in Figure 2.2.2 shows that the local stress field (within $r < a/10$) is given by [Irwin, 1957; Williams, 1957; Sneddon & Lowengrub, 1969; Rice, 1968a]:

$$\sigma_x = \frac{K}{\sqrt{2\pi r}} cos\frac{\theta}{2}\left[1 - sin\frac{\theta}{2} sin\frac{3\theta}{2}\right]$$

$$\sigma_y = \frac{K}{\sqrt{2\pi r}} cos\frac{\theta}{2}\left[1 + sin\frac{\theta}{2} sin\frac{3\theta}{2}\right] \qquad (2.2.1)$$

$$\sigma_{xy} = \frac{K}{\sqrt{2\pi r}} sin\frac{\theta}{2}\left[cos\frac{\theta}{2} cos\frac{3\theta}{2}\right]$$

The stress in the third direction are given by $\sigma_z = \sigma_{xz} = \sigma_{yz} = 0$ for the plane stress problem, and when the third directional strains are zero (plane strain problem), the out of plane stresses become $\sigma_{xz} = \sigma_{yz} = 0$ and $\sigma_z = \nu(\sigma_x + \sigma_y)$. While the geometry and loading of a component may change, as long as the crack opens in a direction normal to the crack path, the crack tip stresses are found to be as given by Equations 2.2.1. Thus, the Equations 2.2.1 only represent the crack tip stress field for the Mode 1 crack extension described by Figure 2.2.2.

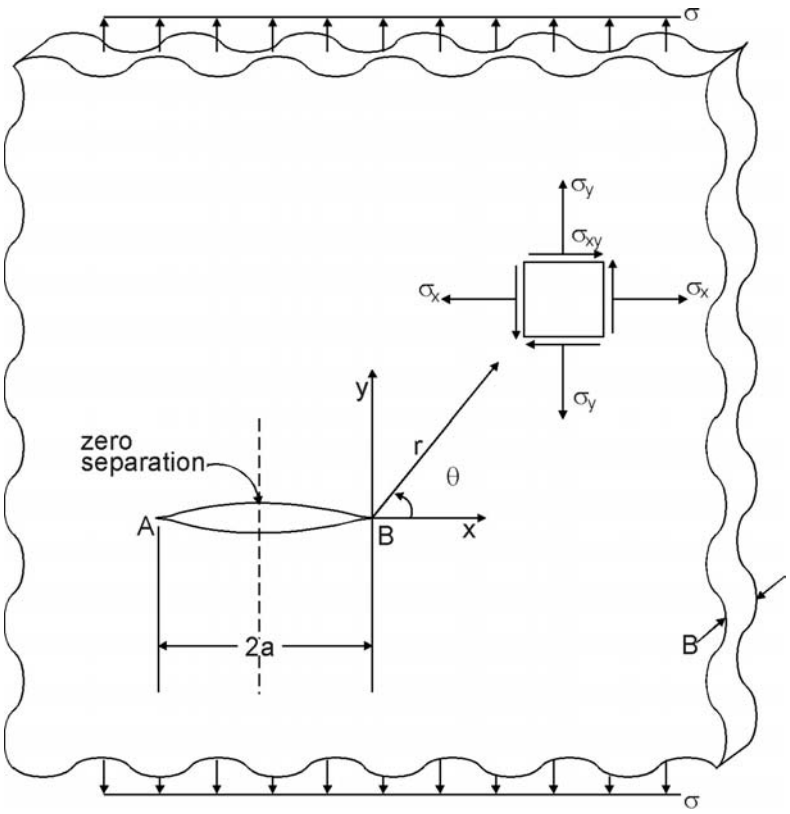

Figure 2.2.2. Infinite Plate with a Flaw that Extends Through Thickness

Three variables appear in the stress field equation: the crack tip polar coordinates r and θ and the parameter K. The functions of the coordinates determine how the stresses vary with distance from the right hand crack tip (point B) and with angular displacement from the x-axis. As the stress element is moved closer to the crack tip, the stresses are seen to become infinite. Mathematically speaking, the stresses are said to have a square root singularity in r. Because most cracks have the same geometrical shape at their tip, the square root singularity in r is a general feature of most crack problem solutions.

The parameter K, which occurs in all three stresses, is called the stress intensity factor because its magnitude determines the intensity or magnitude of the stresses in the crack tip region. The influence of external variables, i.e. magnitude and method of loading and the geometry of the cracked body, is sensed in the crack tip region only through the stress intensity factor. Because the dependence of the stresses (Equation 2.2.1) on the coordinate variables remain the same for different types of cracks and shaped bodies, the stress intensity factor is a single parameter characterization of the crack tip stress field.

The stress intensity factors for each geometry can be described using the general form:

$$K = \sigma\beta\sqrt{\pi a} \tag{2.2.2}$$

where the factor β is used to relate gross geometrical features to the stress intensity factors. Note that β can be a function of crack length (a) as well as other geometrical features

It is seen from Equation 2.2.2 that the intensity of the stress field and hence the stresses in the crack tip region are linearly proportional to the remotely applied stress and proportional to the square root of the half crack length.

A structural analyst should be able to determine analytically, numerically, or experimentally the stress-intensity factor relationship for almost any conceivable cracked body geometry and loading. The analysis for stress-intensity factors, however, is not always straightforward and information for determining this important structural property will be presented subsequently in Section 11. A mini-handbook of stress-intensity factors and some methods for approximating stress-intensity factors are also presented in Section 11.

2.2.2 Application to Fracture

Can the magnitude or intensity of this crack tip pattern be used to characterize the material instability at fracture? The formulation of such a hypothesis for measuring a material's resistance to fracture was developed by G.R. Irwin and his co-workers at the Naval Research Laboratories in the 1950's [Irwin, 1957; Irwin & Kies, 1954; Irwin, et al., 1958].

The hypothesis can be stated:

> if the level of crack tip stress intensity factor exceeds a critical value, unstable fracture will occur.

The concept is analogous to the criterion of stress at a point reaching a critical value such as the yield strength. The value of the stress-intensity factor at which unstable crack propagation occurs is called the fracture toughness and is given the symbol K_c. In equation form, the hypothesis states:

$$\text{if } K = K_c, \tag{2.2.3}$$

then catastrophic crack extension (fracture) occurs.

To verify the usefulness of the proposed hypothesis, consider the results of a wide plate fracture study given in Figure 2.2.3 [Boeing, 1962]. These data represent values of half crack length and gross section stress at fracture. The stress-intensity factor for the uniformly-loaded center-cracked finite-width panel is given by:

$$K = \sigma\left[\pi a \sec\frac{\pi a}{W}\right]^{1/2} \tag{2.2.4}$$

where W is the panel width. Application of Equation 2.2.4 given in Figure 2.2.3 followed by averaging the calculated fracture toughness values (except for those at the two smallest crack lengths) gives the average fracture toughness curve shown. This example illustrates that the fracture toughness concept can be used to adequately describe fractures that initiate at gross sectional stress below 70% of the yield strength.

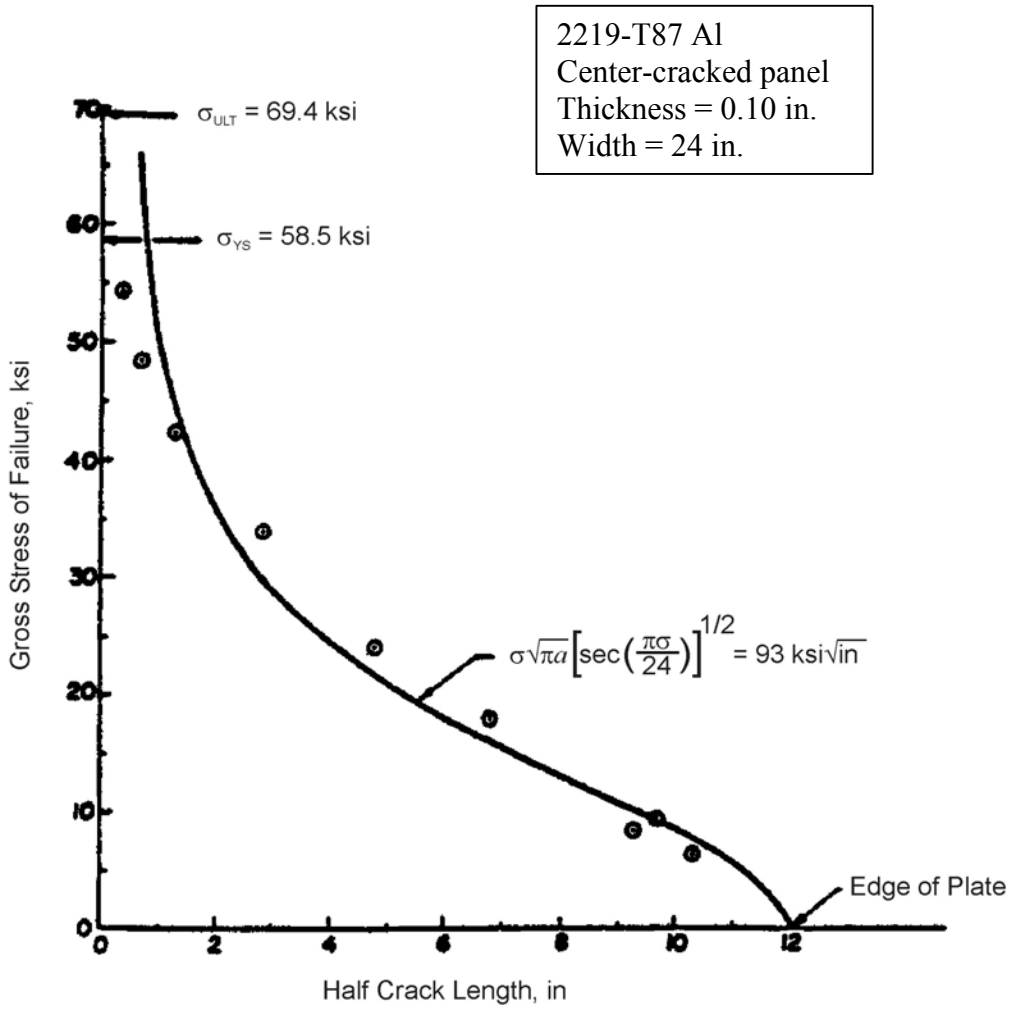

Figure 2.2.3. Results of a Wide Plate Fracture Study Compared with a Fracture Toughness Curve Calculated Using the Finite Width Plate Stress Intensity Factor Equation, Equation 2.2.4 (Data from Boeing [1962])

Note that since plastic deformation is assumed negligible in the linear elastic analysis, Equation 2.2.3 is not expected to yield an accurate approximation where the zone of plastic deformation is large compared to the crack length and specimen dimensions. Figure 2.2.3 shows that the relationship derived on the basis of the Equation 2.2.3 hypothesis does not describe the crack growth behavior for small cracks in plastic stress fields.

2.2.3 Fracture Toughness - A Material Property

Fracture toughness (K_c) is a mechanical property that measures a material's resistance to fracture. This parameter characterizes the intensity of stress field in the material local to the crack tip when rapid crack extension takes place. Similar to other microstructurally sensitive material properties, fracture toughness can vary as a function of temperature and strain rate. But, unlike the yield strength, K_c will be strongly dependent on the amount of crack tip constraint due

to component thickness. The reason why thickness has to be considered in fracture analysis is due to its influence on the pattern of crack tip plastic deformation. The two thickness limiting crack tip plastic deformation patterns are shown in Figure 2.2.4. For "thin" plane stress type components, a 45 degree through the thickness yielding pattern develops; in "thicker" plane strain components of the same material, the hinge-type plastic deformation pattern predominates [Hahn, & Rosenfield, 1965]. Section 4 and 7 discuss the effect of thickness and other factors on fracture toughness.

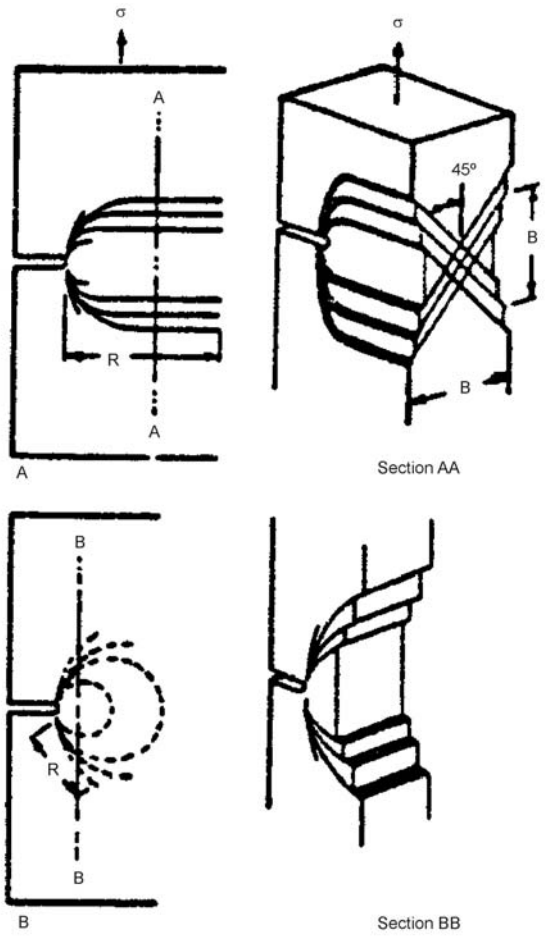

Figure 2.2.4. Yield Zone Observed on the Surface and Cross Section of a Cracked Sheet Under Uni-axial Tensile Loading in: A-Plane Stress, 45 degree Shear Type; B-Plane Strain, Hinge Type

The linear elastic fracture mechanics approach can only be expected to characterize fracture when the region in which plastic deformation occurs is contained within the elastic crack tip stress field. When the crack tip plastic deformation is unrestricted by elastic material around the crack, the engineer must resort to using elasto-plastic techniques to predict the critical crack size at fracture. Presently, it is not possible to say if these techniques will lead to the same type of single parameter characterization of fracture discussed above.

2.2.4 Crack Tip Plastic Zone Size

It is recognized that plastic deformation will occur at the crack tip as a result of the high stresses that are generated by the sharp stress concentration. To estimate the extent of this plastic deformation, Irwin equated the yield strength to the y-direction stress along the x-axis and solved for the radius. The radius value determined was the distance along the x-axis where the stress perpendicular to the crack direction would equal the yield strength; thus, Irwin found that the extent of plastic deformation was

$$r_y = \frac{1}{2\pi}\left(\frac{K}{\sigma_{ys}}\right)^2 \qquad (2.2.5)$$

Subsequent investigations have shown that the stresses within the crack tip region are lower than the elastic stresses and that the size of the plastic deformation zone in advance of the crack is between r_y and $2r_y$. Models of an elastic, perfectly plastic material have shown that the material outside the plastic zone is stressed as if the crack were centered in the plastic zone. Figure 2.2.5 describes a schematic model of the plastic zone and the stresses ahead of the crack tip. Note that the real crack is blunted as a result of plastic deformation.

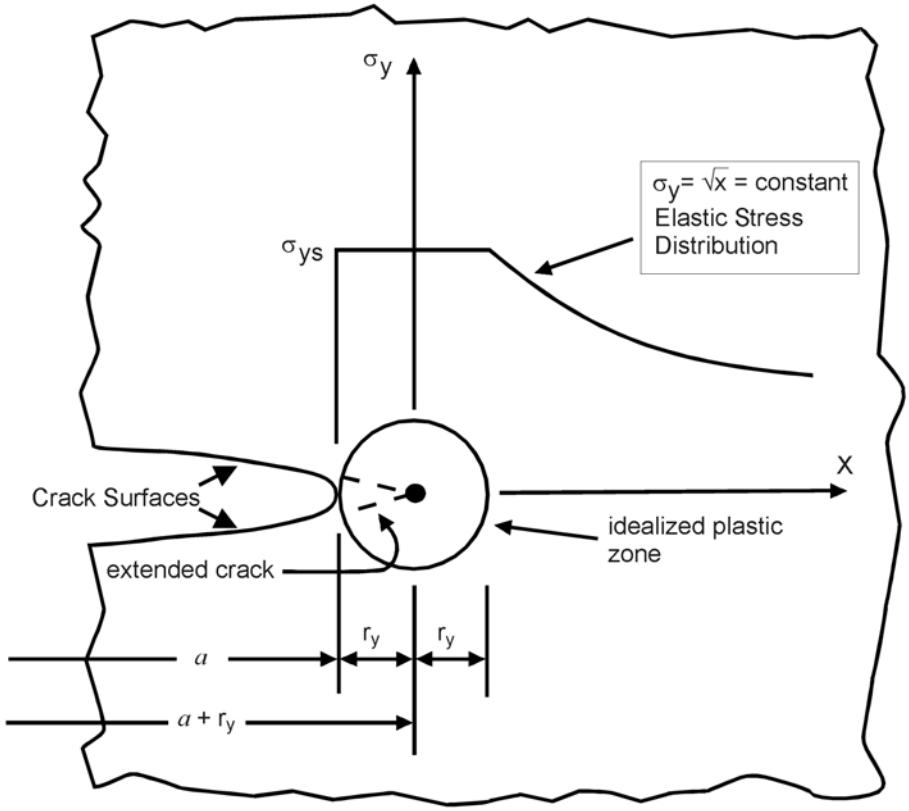

Figure 2.2.5. Small-Scale Yield Model for Restricted Crack Tip Plastic Deformation

If the extent of the plastic zone as estimated by Equation 2.2.5 is small with respect to features of the structural geometry and to the physical length of the crack, linear elastic fracture mechanics analyses apply. Sometimes, the concept of contained yielding, as illustrated in Figure 2.2.5, is referred to as small scale yielding. Most structural problems of interest to the aerospace community can be characterized by linear elastic fracture mechanics parameters because the extent of yielding is contained within a small region around the crack tip.

2.2.5 Application to Sub-critical Crack Growth

The only quantifiable measure of sub-critical damage is a crack. Cracks impair the load-carrying characteristics of a structure. As described above, a crack can be characterized for length and configuration using a structural parameter termed the stress intensity factor (K). This structural parameter was shown to interrelate the local stresses in the region of the crack with crack geometry, structural geometry, and level of load on the structure. In a manner similar to Irwin, who utilized the stress intensity factor for fracture studies, Paris and his colleagues at Lehigh University and at the Boeing Company developed a crack mechanics approach to solve sub-critical crack growth problems [Paris, et al., 1961; Donaldson & Anderson, 1961; Paris, 1964].

The concepts that Paris and his colleagues developed were based upon a similitude hypothesis: if the crack tip stress state and its waveform are the same in a given time period for two separate geometry and loading conditions, then the crack growth rate behavior observed by the two cracks should be the same for that time period. This hypothesis is a direct extension of Equation 2.2.3 to the problem of sub-critical crack growth. The equation representing the sub-critical crack growth hypothesis is simply:

$$\frac{\Delta a}{\Delta t} = f(K(t))$$

or (2.2.6)

$$\frac{\Delta a}{\Delta N} = f(K(t))$$

That is, a material's rate of crack growth is a function of the stress intensity factor. The stress intensity factor is shown to explicitly depend on time in order to indicate the influence of its waveform on the crack growth rate. The value of the hypothesis stated by Equation 2.2.6 is that the material behavior can be characterized in the laboratory and then utilized to solve structural cracking problems when the structure's loading conditions match the laboratory loading conditions. A general description of the procedure utilized will be presented in Section 2.5. Section 5 is devoted to a complete description of the detailed methodology available to a designer for estimating the crack growth life of a structural component using a material's crack growth rate properties.

A verification of Paris' Hypothesis was first conducted using fatigue crack growth data generated under constant amplitude type repeated loading. The parameters that pertain to constant amplitude type loading are presented in Figure 2.2.6. Figure 2.2.6a describes a repeating constant amplitude cycle with a maximum stress of σ_{max}, a minimum stress of σ_{min}, and a stress range of $\Delta\sigma$. The stress ratio (R) is given by the ratio of the minimum stress to the maximum stress. In describing constant amplitude stress histories, it is only necessary to define two of the above four parameters; typically $\Delta\sigma$ and R or σ_{max} and R are used. A stress history is

converted into a stress-intensity factor history by multiplying the stresses by the stress-intensity-factor coefficient (K/σ). As can be noted from the figure, the coefficient is evaluated at the current crack length a_i and the stress-intensity-factor history is shown to be a repeating cyclic history in Figure 2.2.6b. The terms K_{max}, K_{min} and ΔK define the maximum, the minimum and range of stress-intensity factor, respectively. Strictly speaking, the stress-intensity factor history given in Figure 2.2.6b should not be shown constant but reflective of the changes in the stress-intensity-factor coefficient as the crack grows. For small changes in crack length, however, the stress-intensity factor coefficient does not change much, so the portrayal in Figure 2.2.6b is reasonably accurate for the number of cycles shown.

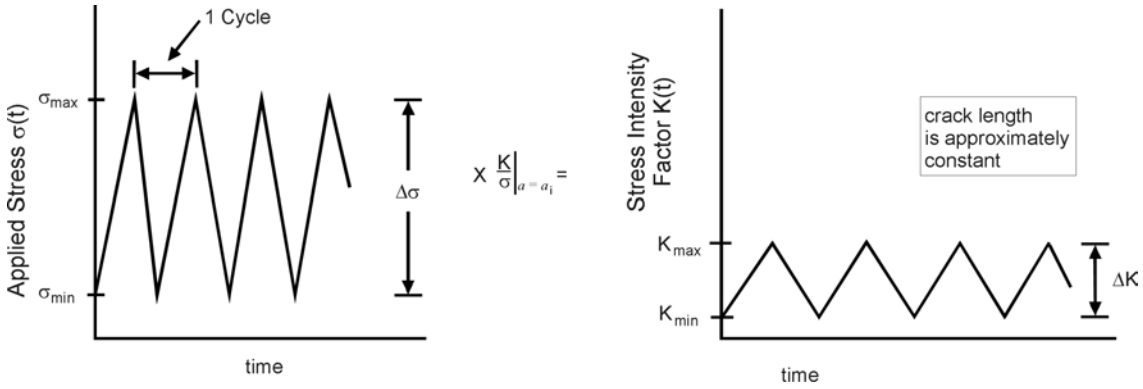

Figure 2.2.6. Parameters that Define Constant Amplitude Load Histories for Fatigue Crack Growth. The Figure also Illustrates the Transformation between Stress History Loading and Stress-Intensity-Factor Loading at One Crack Length Position

The fatigue crack growth rate behaviors exhibited by a plate structure subjected to two extreme loading conditions (but at the same nominal stress level) are compared in Figure 2.2.7 [Donaldson & Anderson, 1961; Anderson & James, 1970]. These loading conditions are referred to as wedge loading and remote loading. In the remote loaded structure, the rate of crack length change accelerates as the crack grows. An opposite growth rate behavior is exhibited by the wedge loaded structure. These two extreme loading conditions provide a good test for the application of the fracture mechanics approach to the study of fatigue crack growth rates. If the approach can be used to describe these opposite growth rate behaviors, then it should be generally applicable to any other type of structure or loading.

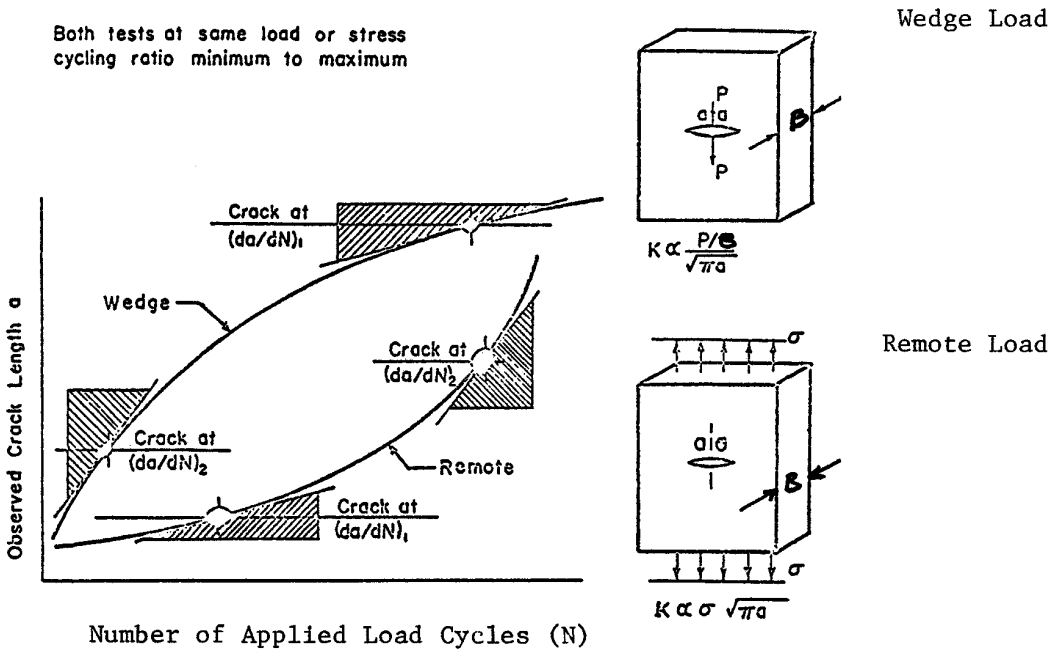

Figure 2.2.7. Description of Crack Growth Behavior Observed for Two Very Different Structural Geometries

Paris, et al. [1961], suggested that the appropriate stress intensity parameter for fatigue crack propagation should be the difference between the maximum and minimum stress-intensity factors in a cycle of fatigue loading. This difference in the stress-intensity factors is the stress intensity range *(ΔK)* and it measures the alternating intensity of the crack tip stress field responsible for inducing reversed plastic deformation. The stress-intensity range as a function of crack length is obtained from the static stress-intensity-factor formulas where the range in stress (load) replaces the static stress (load). Section 2.5 provides a more extensive description of the calculation procedures for stress-intensity-factor parameters that are used to describe sub-critical crack growth.

Approximate expressions for the small crack in a wide plate are shown in Figure 2.2.7. The reader will note that the stress-intensity factor for the remotely loaded wide plate increases with crack length while just the reverse is observed to occur for the wedge loaded wide plate.

Drawing tangents to the cyclic crack length curves given in Figure 2.2.7 provides estimates of the cyclic (fatigue) crack growth rates at various crack lengths $\left(\frac{da}{dN} \cong \frac{\Delta a}{\Delta N}\right)$. Calculation of corresponding stress-intensity ranges for these same crack lengths provides the data plotted in Figure 2.2.8 [Donaldson & Anderson, 1961; Anderson & James, 1970]. Note that at the same stress-intensity range *(ΔK)*, the same crack growth rate (*da/dN*) is observed, even though both the form of the stress-intensity equations and the cycle-crack length curves are very different.

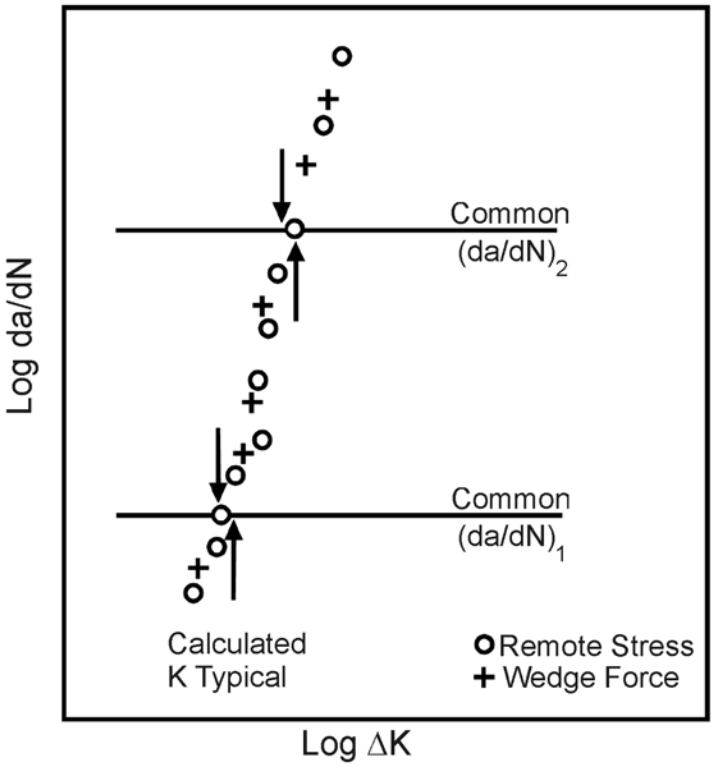

Figure 2.2.8. Comparison of Crack Growth Rate Results for the Two Structural Geometries. The Coincidence of the Data Shows that the Hypothesis of Equation 2.2.6 is Correct

The general fatigue cracking behavior pattern exhibited by most structural materials is shown in Figure 2.2.9. The shape of the curve is sigmoidal with no crack growth being observed below a given threshold level of stress-intensity range and rapid crack propagation occurring when the maximum stress-intensity-factor in the fatigue cycle approaches the fracture toughness of the material. In the sub-critical growth region, numerous investigators have indicated that the rate of cyclic growth (*da/dN*) can be described using a power law relation

$$\frac{da}{dN} = C(\Delta K)^p \qquad (2.2.7)$$

where C and p are experimentally developed constants. Fatigue crack propagation data of the type shown in Figure 2.2.9 can be conveniently collected using the conventional specimen geometries where load is controlled and the crack length is measured optically (20x) as a function of applied cycles. The details of the methodology employed to generate such curves are covered in Section 7.

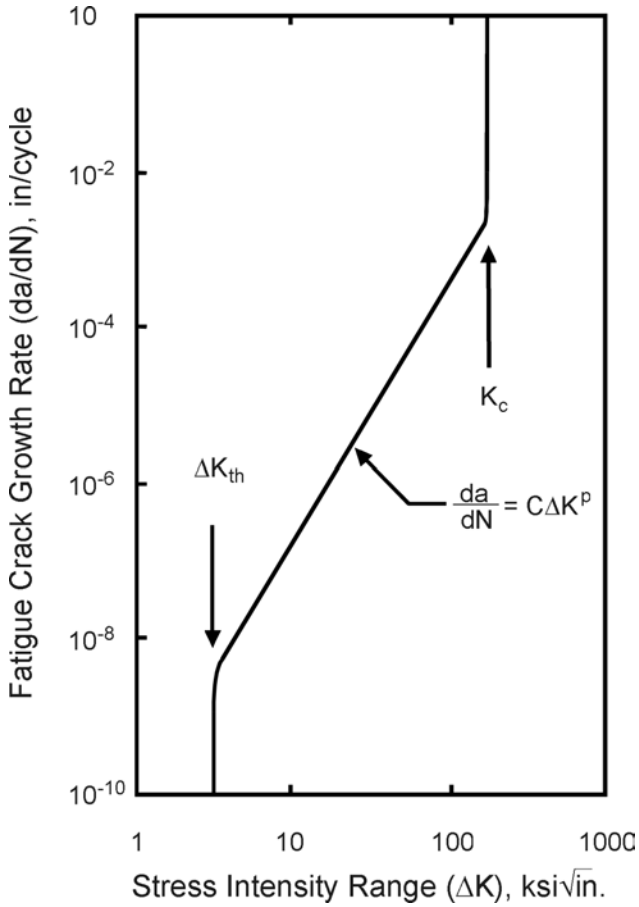

Figure 2.2.9. Schematic Illustration of the Fatigue Crack Growth Rate as a Function of Stress Intensity Range

The application of sub-critical crack growth curves to the design of a potentially cracked structure only requires that the differentiation process be reversed. In other words, given crack growth rate data of the type shown in Figure 2.2.9, the designer integrates the crack growth rate as a function of the stress-intensity factor for the structure through the crack growth interval of interest.

Other investigations have demonstrated that sub-critical crack growth processes that result from variable amplitude loading, stress corrosion cracking, hydrogen embrittlement and liquid metal embrittlement can in general be described using Equation 2.2.6. The sub-critical cracking of structural materials has been successfully modeled with fracture mechanics tools primarily because the plastic deformation processes accompanying cracks are localized and thereby controlled by the surrounding stress field. As suspected, the magnitude in the elastic crack tip stress field is found to correlate well with the rate of sub-critical crack advance.

2.2.6 Alternate Fracture Mechanics Analysis Methods

In the other subsections of Section 2, the emphasis has been on developments of linear elastic fracture mechanics (LEFM) specifically based on the crack tip characterizing parameter *K*, the stress-intensity factor. This parameter has provided the major damage tolerance design tool for aerospace engineers since the early sixties. It was discovered and justified for its universal

capability for describing the magnitude of the crack tip stress field by Irwin [1957; 1960] and Williams [1957]. Irwin discovered this relationship through his studies of the energy balance equation associated with fracture. Prior to 1957, fracture research concentrated on extending the original energy balance equation given by Griffith [1921] In 1957, Irwin [1960] linked the "driving force", G, in the energy balance equation to the stress-intensity factor, K, and suggested how the stress-intensity factor could be used as the driving force for crack tip behavior. Subsequent to Irwin's initial stress-intensity factor analysis, and as a result of the success of the LEFM approach for solving major fracture problems, interest in the energy approach to fracture waned.

In the late sixties, Rice [1968b] published a paper that again heightened the interest in the energy approach. Rice's specific contribution was to develop an integral, the J-integral, which could be used to account for observed non-linear behavior during the fracture process. This integral also has the useful property that it reduces to the elastic "driving force", G, when the localized plastic deformation is well contained by the elastic crack tip stress field. Because many of the materials utilized in aerospace structures have exhibited typical LEFM behavior, aerospace engineers have not assumed a leadership role in the development of the J-integral technology.

Engineers interested in the damage tolerance analysis of more ductile pressure vessels and welded steel structures have provided the major developments here. Aerospace applications are being recognized each day, however, for this technology, e.g., residual strength analysis of tough materials and sub-critical crack growth behavior of aircraft gas turbine engine structures.

Another analysis approach for characterizing the level of the local stress-strain behavior at the tip of a crack was initiated in Britain in the early sixties. Wells [1961] suggested that the localized behavior at the tip of the crack was controlled by the amount of crack opening, which was referred to as the crack opening displacement, COD. The value of the technology built on the COD concept, like that of the J-Integral technology, is that it allows for the coupling of the LEFM analysis and its results to the solution of problems in which the behavior approaches unconstrained yielding.

The subsections below further describe the analysis methodologies based on the three fracture mechanics parameters: the strain energy release rate (driving force - G), the J-Integral (J), and the crack opening displacement (COD), respectively. Each subsection outlines the analytical basis for the parameter and provides the principal equations that tie the parameter to the LEFM parameter K. Further information on these parameters can be obtained by the references cited in the text.

2.2.6.1 Strain Energy Release Rate

Paris [1960] gave one of the better descriptions of the fracture energy balance equation associated with the stability of a cracking process in a set of notes prepared for a short course given to the Boeing Company in 1960. Paris simply described the process of determining if a crack would extend as a comparison between the Rate of Energy Input and the Rate at which Energy was absorbed or dissipated. This comparison is similar to performing as analysis based on the Principle of virtual work. In equation form, Paris indicated

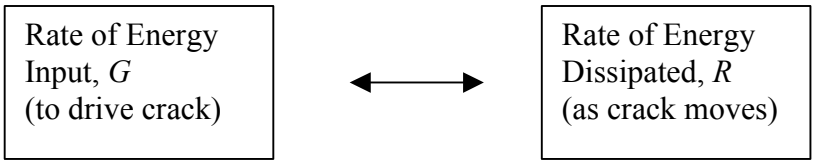

(2.2.8)

where the left hand side of Equation 2.2.8 represents the input rate (as a function of crack area A) and the right hand side represents the dissipation rate. If the input rate, the driving force G, is equal to the dissipation rate, the resistance R, then the crack is in an equilibrium (stable) position, i.e., it is ready to grow but doesn't. If the driving force exceeds the resistance, then the crack grows, an unstable position. Since a crack will not heal itself, if the resistance is greater than the driving force, then the crack is also stable.

The basis for Equation 2.2.8 was further described [Paris, 1960] so that the components are identified as:

$$G = \frac{dX}{dA} + \frac{dG}{dA} \lessgtr \frac{dS}{dA} + \frac{dQ}{dA} = R \qquad (2.2.9)$$

where < and = imply stability while > implies instability.

The driving force (input work rate, G) components are:

$\frac{dX}{dA}$ = the work done by external forces on the body unit increase in crack area, dA.

$\frac{dG}{dA}$ = the elastic strain energy released per unit increase in dA.

And the resistance (rate of dissipation, R) components are:

$\frac{dS}{dA}$ = surface energy absorbed in creating a new surface area, dA.

$\frac{dQ}{dA}$ = plastic work dissipated throughout the body during an increase in surface area, dA.

While Equation 2.2.9 is most general and covers fractures that initiate in either brittle or ductile materials, it is not always possible to estimate the individual component terms. For linear elastic materials, the terms can be estimated; and in fact, this was accomplished by Griffith [1921] forty years before Paris presented the above general work rate analysis in 1960. Before any further discussion of the work preceeding that of Paris, however, several additional points need to be made about Equation 2.2.9. First, the component terms of the input energy rate will be defined relative to a specific structural geometry and loading configuration: the uniaxially loaded, center cracked panel shown in Figure 2.2.10. Then the input energy rate (G) will be related to the elastic strain energy.

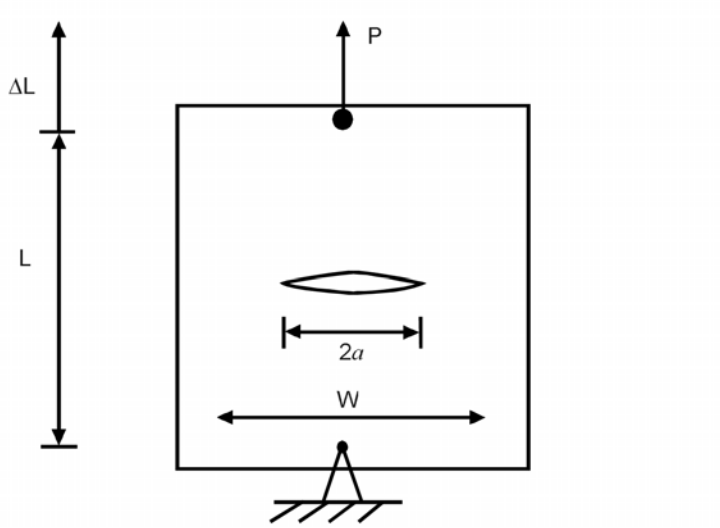

Figure 2.2.10. Finite Width, Center Cracked Panel, Loaded in Tension with Load *P*

The two components of the energy input rate (G) are given by

$$\frac{dX}{dA} = \frac{PdL}{dA} \tag{2.2.10}$$

the boundary force per increment of crack extension; and by

$$\frac{dG}{dA} = \frac{-dV}{dA} \tag{2.2.11}$$

the decrease in the total elastic strain energy of the plate. With these additional definitions, it can be seen that G is equal to the negative of the rate of change in the potential energy of deformation (U_σ), i.e.,

$$G = \frac{-dU_\sigma}{dA} \tag{2.2.12}$$

2.2.6.1.1 The Griffith-Irwin Energy Balance

The earliest analysis along the above lines was conducted by Griffith [1921] in 1920. Griffith used the crack geometry and loading configuration shown in Figure 2.2.11 and assumed that the stress would be constant during any incremental growth of the crack. Griffith also neglected the plastic work term in Equation 2.2.9 since he was trying to test his fracture hypothesis with a brittle material, glass. Griffith's analysis showed that the input work rate (G) was equal to the negative of the derivative of potential energy of deformation (U_σ) as shown by Equation 2.2.12, and the resistance (R) was equal to the rate of increase in potential energy due to surface energy (U_T) during crack extension:

$$R = \frac{dS}{dA} = \frac{dU_T}{dA} \tag{2.2.13}$$

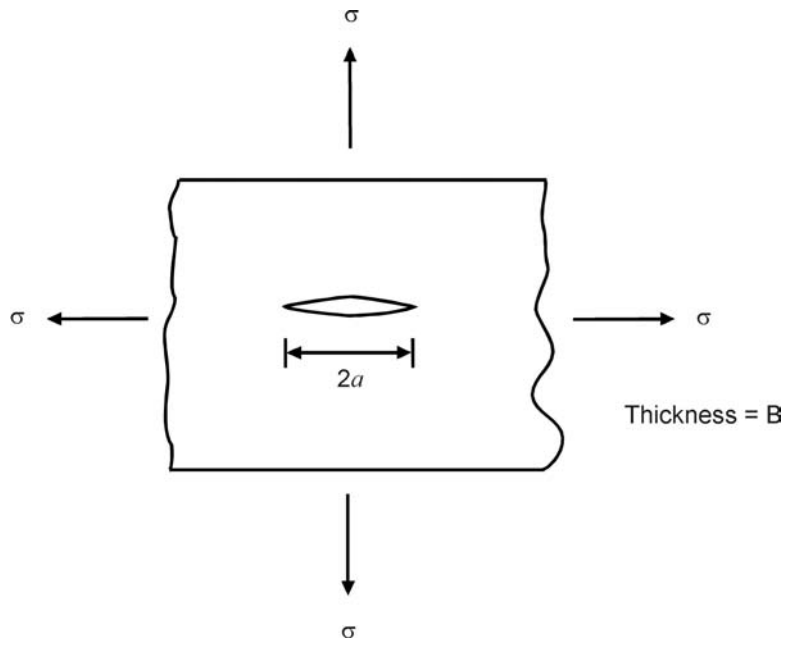

Figure 2.2.11. Griffith Crack and Loading Configuration, Uniformly Loaded, Infinite Plate with a Center Crack of Length 2*a*

The potential energy of deformation (U_σ) was found to be

$$U_\sigma = \frac{\pi\sigma^2 a^2 B}{E} \tag{2.2.14}$$

while the potential energy due to surface tension (U_T) was given by

$$U_T = 4aTB \tag{2.2.15}$$

with surface tension T, and for plate thickness B.

The crack area A is given by

$$A = 2aB \tag{2.2.16}$$

So the energy balance equation becomes

$$G = \frac{-dU}{dA} = \frac{\sigma^2 \pi a}{E'} = 2T = \frac{dS}{dA} = R \tag{2.2.17}$$

where E′ is dependent on the stress state in the following way

$$E' = \begin{cases} E/(1-\nu^2), \text{ for plane strain} \\ E, \text{ for plane stress} \end{cases} \tag{2.2.18}$$

Solving Equation 2.2.17 for the critical stress (σ_{cr}) associated with the point at which the crack (a) would grow, one finds

$$\sigma_{cr} = \sqrt{\frac{2TE'}{\pi a}} \tag{2.2.19}$$

Later, Irwin [1948] and Orowan [1949] incorporated the effects of crack tip plasticity into the analysis by taking the plastic dissipation term in Equation 2.2.9 as a constant, i.e. they assumed that

$$\frac{dQ}{dA} = q \tag{2.2.20}$$

so that the resistance in Equation 2.2.17 was defined as the combination of surface energy absorbed and plastic work dissipated. Thus, the Griffith-Irwin-Orowan energy balance equation became

$$G = \frac{\sigma^2 \pi a}{E'} = 2T + q = R \tag{2.2.21}$$

and the critical stress was

$$\sigma_{cr} = \sqrt{\frac{(2T + a)E'}{\pi a}} \tag{2.2.22}$$

Both Irwin and Orowan noted that the plastic dissipation rate for metals was at least a factor of 1000 greater than the surface energy absorption rate so that Equation 2.2.22 could be approximated by

$$\sigma_{cr} = \sqrt{\frac{qE'}{\pi a}} \tag{2.2.23}$$

Irwin also noted that the driving force or input energy rate G was directly related to the square of the magnitude of the crack tip stress field for the Griffith center crack geometry (Figure 2.2.11), i.e., that

$$G = \frac{\sigma^2 \pi a}{E'} = \frac{K^2}{E'} \tag{2.2.24}$$

Later, Irwin [1960] reported this result to be general for any cracked elastic body based upon a virtual work analysis of the stresses and displacements associated with crack tip behavior during an infinitesimal crack extension.

2.2.6.1.2 The Relationship between G, Compliance, and Elastic Strain Energy

If one defines the relationship between the force (P) applied to the structure shown in Figure 2.2.10 and the deformation it induces in the direction of load as

$$\Delta L = C \cdot P \tag{2.2.25}$$

where

$$C = C(A) \tag{2.2.25a}$$

is the compliance, the inverse structural stiffness, which varies as a function of crack length (area). With the definitions given by Equation 2.2.25, the elastic strain energy (V) can be written as

$$V = \frac{P.\Delta L}{2} = \frac{CP^2}{2} \tag{2.2.26}$$

The change in V simultaneous to dA and dP is

$$dV = \frac{\partial V}{\partial A}\Big|_P dA + \frac{\partial V}{\partial P}\Big|_A dP \tag{2.2.27}$$

which leads to

$$dV = \frac{P^2}{2}\frac{\partial C}{\partial A}dA + CPdP \tag{2.2.28}$$

Similar operations on changes in dL $(=d(\Delta L))$ lead to

$$PdL = P^2\frac{\partial C}{\partial A}dA + PCdP \tag{2.2.29}$$

So that the input energy rate (G) based on Equation 2.2.9 becomes

$$G = \frac{dX}{dA} + \frac{dG}{dA} = \frac{P^2}{2}\cdot\frac{\partial C}{\partial A} + (0)\cdot\frac{dF}{dA} \tag{2.2.30}$$

Showing that the input energy rate is independent of the variation of force during any incremental crack extension. Thus, Equation 2.2.30 reduces to

$$G = \frac{P^2}{2}\frac{\partial C}{\partial A} \equiv \frac{\partial V}{\partial A}\Big|P = constant \tag{2.2.31}$$

Equation 2.2.31 provides the basis for experimentally evaluating the crack driving force using compliance measurements and clearly shows that the rate of energy input is identically equal to the change in elastic strain energy considering the loading force constant. When one conducts a similar analysis with the displacement (Δ) and crack area (A) as independent variables, one finds that

$$G = -\frac{\partial V}{\partial A}\Big|\Delta L = constant \tag{2.2.32}$$

which means that the input energy rate is the negative of the areal derivative of elastic strain energy considering the displacement constant during crack extension. This is the so-called fixed displacement condition. The term strain energy release rate was assigned to G, the input energy rate, when it was realized that for cracked elastic bodies Equation 2.2.30 and 2.2.31 were generally applicable.

Figure 2.2.12 describes the change in elastic strain energy that occurs when a crack grows under fixed load and fixed displacement conditions. It can be noted that the difference between the change in elastic strain energy for the two cases is the infinitesimal area $\frac{1}{2}dP * \Delta L$, shown cross-

hatched in Figure 2.2.12a. For the case of the fixed load condition (Figure 2.2.12a), the elastic strain energy is seen to increase as the crack grows; the gain in elastic strain energy is greater than the indicated loss (by a factor of 2). For the case of the fixed displacement condition (Figure 2.2.12b), the elastic strain energy is seen to decrease as the crack grows; only a loss is indicated.

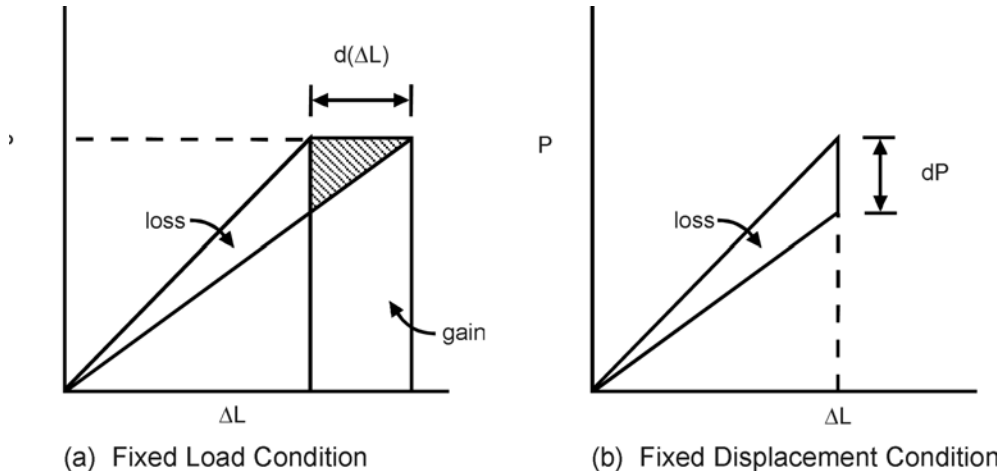

Figure 2.2.12. Load-Displacement Diagrams for the Structure Illustrated in Figure 2.2.10. The Diagram Shows the Changes that Occur in the Elastic Strain Energy as a Crack Grows Under the Two Defined Conditions

Some important observations presented in the subsection are:

(a) the general form of Equation 2.2.24 can be utilized to relate G and K;

(b) G is equal to the negative rate of change in the potential energy of deformation (Equation 2.2.12); and

(c) G is related to the areal rate of change in compliance (Equation 2.2.31).

Note that by combining Equations 2.2.24 and 2.2.12 or 2.2.31 the analyst and/or experimentalist have energy-based methods for obtaining estimates of the stress-intensity factor. These combinations are discussed in Section 11.2.1.4 (see, for example, Equation 11.2.25).

2.2.6.2 The J-Integral

In 1968, Rice [1968b] published a paper describing a path independent integral (J) which was noted to be equal to the negative of the change in potential energy of deformation occurring during the infinitesimal growth of a crack in a nonlinear elastic material, i.e. he showed that

$$J = -\frac{\partial U_\sigma}{\partial A} \tag{2.2.33}$$

Rice's path independent integral J was defined by [Rice, 1968a; 1968b]

$$J = \int_{\Gamma} \left(W dy - \vec{T} \cdot \frac{\partial \vec{u}}{\partial x} ds \right) \tag{2.2.34}$$

where Γ is any contour surrounding the crack tip, traversing in a counter clockwise direction (see Figure 2.2.13), W is the strain energy density, $\vec{\Gamma}$ is the traction on Γ, and $\vec{u}$ is the displacement on an element along arc s.

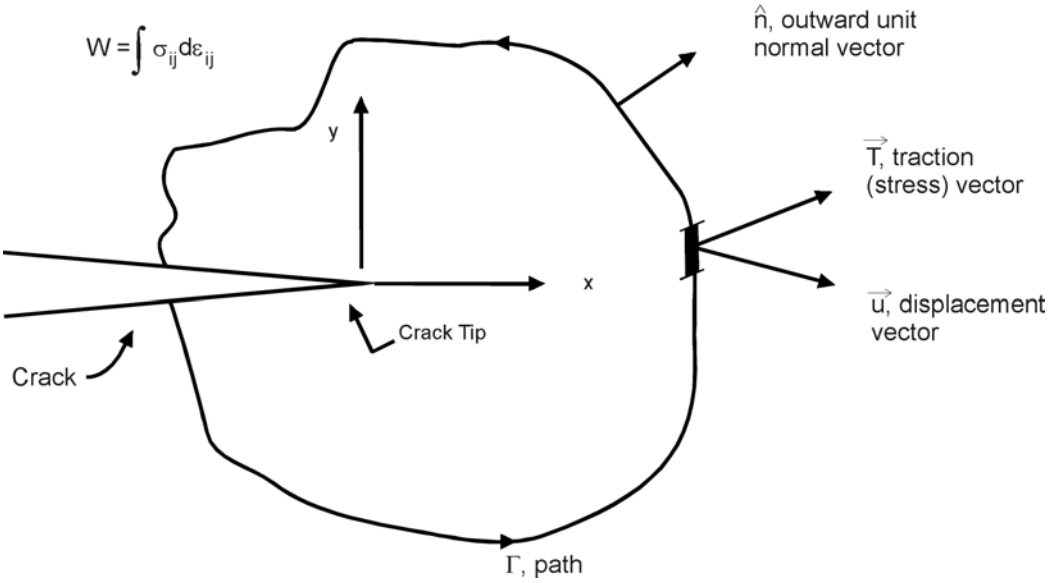

Figure 2.2.13. *J*-Integral Parameters Illustrated

Before elaborating on a detailed description of the parameters involved in the calculation of the *J*-Integral, it is useful to note that Equation 2.2.33 is the nonlinear elastic equivalent of Equation 2.2.12. Thus, for linear elastic materials, *J* reduces to the value of the strain energy release rate, *G*, i.e.

$$J = G \tag{2.2.35}$$

and the *J*-integral is related to the stress-intensity factor through the expression

$$J = \frac{K^2}{E'} \tag{2.2.36}$$

where E' is given by Equation 2.2.18.

Equations 2.2.35 and 2.2.36 are noted to be valid only when the material is behaving in a linear elastic fashion. When values of the *J*-Integral are determined via Equation 2.2.34 using finite element methods applied to linear elastic cracked structures, Equation 2.2.36 provides the engineer with a simple energy-based method for obtaining stress-intensity factors as a function of crack length.

In the first subsection below, the calculations associated with developing the *J*-Integral for an elastic-plastic material are detailed. In the second subsection, some engineering approximation methods for calculating the J-Integral are outlined.

2.2.6.2.1 J-Integral Calculations

This subsection outlines the calculation of parameters involved in the *J*-Integral. Consideration is given to W, $\vec{T}, \vec{u}$, and Γ as well as the choice of material stress-strain behavior.

The strain energy density W in Equation 2.2.34 is given by

$$W = \int \left[\sigma_{xx} d\varepsilon_{xx} + \sigma_{xy} d\gamma_{xy} + \sigma_{xz} d\gamma_{xz} + \sigma_{yy} d\varepsilon_{yy} + \sigma_{yz} d\gamma_{yz} + \sigma_{zz} d\varepsilon_{zz}\right] \qquad (2.2.37)$$

and for generalized plane stress

$$W = \int \left[\sigma_{xx} d\varepsilon_{xx} + \sigma_{xy} d\gamma_{xy} + \sigma_{yy} d\varepsilon_{yy}\right] \qquad (2.2.38)$$

In Equation 2.2.34, the second integral involves the scalar product of the traction stress vector $\vec{\boldsymbol{T}}$ and the vector $\dfrac{\partial \vec{u}}{\partial x}$ whose components are the rate of change of displacement with respect to x. The traction vector is given by

$$\vec{T} = T_x \hat{i} + T_y \hat{j} = \left(\sigma_{xx} \cdot n_x + \sigma_{xy} n_y\right)\hat{i} + \left(\sigma_{yx} \cdot n_x + \sigma_{yy} \cdot \sigma_{yy} n_y\right)\hat{j} \qquad (2.2.39)$$

and the displacement rate vector is given by

$$\frac{\partial \vec{u}}{\partial x} = \frac{\partial u}{\partial x}\hat{i} + \frac{\partial v}{\partial x}\hat{j} \qquad (2.2.40)$$

where u and v are the displacements in the x and y directions, respectively.

Typically, when evaluating the *J*-Integral value via computer, rectangular paths such as the one illustrated in Figure 2.2.14 are chosen. Noted on Figure 2.2.14 are the values of the outward unit normal components and the *ds* path segment for the four straightline segments. For loading symmetry about the crack axis (x-axis), the results of the integration on paths 0-1, 1-2 and 2-3 are equal to the integrations on paths 6-7, 5-6 and 4-5, respectively. Thus, for such loading symmetry, one can write

$$\begin{aligned} J = 2\Bigg\{ & \int_6^7 \left[W - \sigma_{xx}\frac{\partial u}{\partial x} - \sigma_{xy}\frac{\partial v}{\partial x}\right] dy + \int_5^6 \left[\sigma_{xy}\frac{\partial u}{\partial x} + \sigma_{yy}\frac{\partial v}{\partial x}\right] dx \Bigg\} \\ & + \int_4^5 \left[W - \sigma_{xx}\frac{\partial u}{\partial x} - \sigma_{xy}\frac{\partial v}{\partial x}\right] dy \end{aligned} \qquad (2.2.41)$$

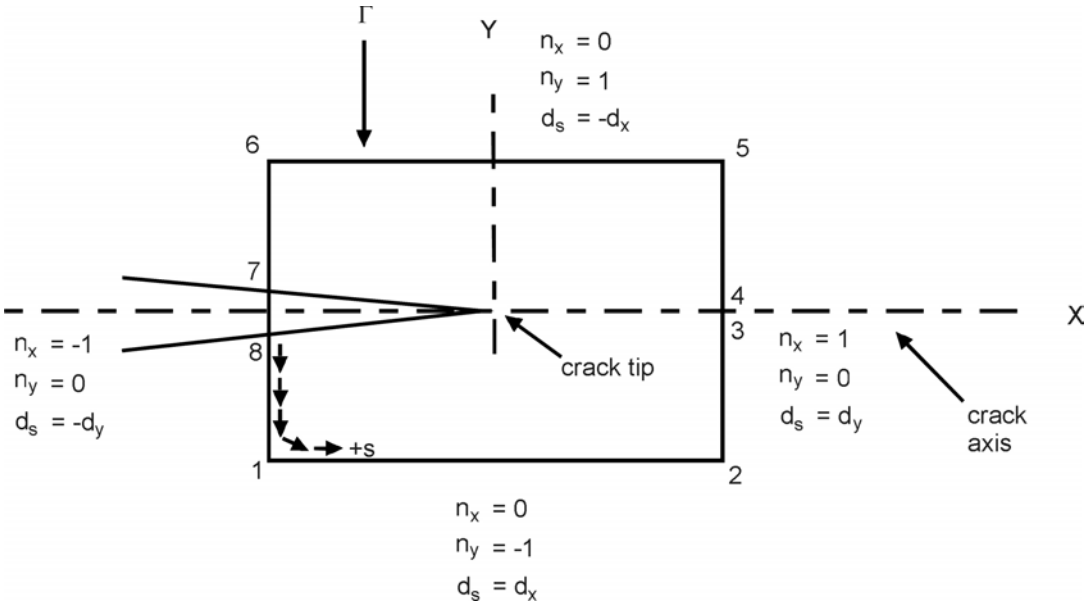

Figure 2.2.14. Rectangular Path for *J* Calculation

For paths of the type shown in Figure 2.2.14, the *J*-Integral can be evaluated by the integrations indicated in Equation 2.2.41. The strain energy density *W*, appearing in Equation 2.2.41, is given by Equation 2.2.37, or by Equation 2.2.38 for plane stress conditions. To integrate according to Equations 2.2.37 or 2.2.38, a relationship between stresses and strains is required. For material exhibiting plastic deformations, the Prandtl-Reuss equations provide a satisfactory relationship. For the case of plane stress, when the Prandtl-Reuss relations are introduced into Equation 2.2.38, Equation 2.2.38 becomes

$$W = \frac{1}{2E}\left[\sigma_{xx} + \sigma_{yy}\right]^2 + \frac{(1-\upsilon)}{E}\left[\sigma_{xy}{}^2 - \sigma_{xy}\sigma_{yy}\right] + \int \bar{\sigma} d\bar{\varepsilon}_p \qquad (2.2.42)$$

where $\bar{\sigma}$ and $\bar{\varepsilon}_p$ are the equivalent stress and equivalent plastic strain, respectively. The strain energy density will have a unique value only if unloading is not permitted. If loading into the plastic range followed by unloading is permitted, then W becomes multi-valued. It follows that *J* is also multi-valued for this occurrence.

The statements made in the preceding paragraph would appear to seriously limit the use of *J* as a fracture criterion since the case of loading into the plastic range followed by unloading (i.e., the case for which *J* is multi-valued) occurs when crack extension takes place. On the basis of a number of examples, Hayes [1970] deduced that monotonic loading conditions prevail throughout a cracked body under steadily increasing load applied to the boundaries, provided that crack extension does not occur. Thus, valid *J* calculations can be performed for this case.

2.2.6.2.2 Engineering Estimates of J

While the J-Integral was developed for nonlinear elastic material behavior, it has been extensively studies for its direct application to describing elastic-plastic material behavior [Begley & Landes, 1972; Verette & Wilhem, et al., 1973; Landes, et al., 1979; Paris, 1980; Roberts, 1981]. Its nonlinear elastic foundation has provided engineers with some techniques

which allow them to focus on the combination of linear-elastic and plastic-strain hardening behavior and then to separate these two components for further study of the plastic behavior. The *J*-Integral for an elastic-plastic material is taken as the sum of two components parts: the linear elastic part (J_{el}) and the plastic-strain hardening part (J_{pl}), i.e.,

$$J = J_{e\ell} + J_{p\ell} \tag{2.2.43}$$

which when used in conjunction with Equation 2.2.36 becomes

$$J = \frac{K^2}{E'} + J_{p\ell} \tag{2.2.44}$$

Engineering estimates of *J* then focus on the development of the plastic-strain hardening part J_{pl}. Recently, Shih and coworkers have published a series of reports and technical papers [Shih & Kumar, 1979; Kumar, et al., 1980; Shih, 1976; Kumar, et al., 1981] detailing how the J_{pl} term can be calculated from a series of finite element models that consider changes in material properties for the same structural geometry. The following briefly describes the Shih and coworkers method for estimating J_{pl}.

First, the material is assumed to behave according to a power hardening constitutive (σ - ε) law of the form

$$\frac{\varepsilon}{\varepsilon_o} = \alpha\left(\frac{\sigma}{\sigma_o}\right)^n \tag{2.2.45}$$

where α is a dimensionless constant, $\sigma_o = E\varepsilon_o$, and n is the hardening exponent. For $n = 1$, the material behaves as a linearly elastic material; as *n* approaches infinity, the material behaves ore and more like a perfectly plastic material. For a generalization of Equation 2.2.45 to multiaxial states via the J_2 deformation theory of plasticity, Ilyushin [1946] showed that the stress at each point in the body varies linearly with a single load such as σ, the remotely applied stress, under certain conditions.

Ilyushin's analysis allowed Shih and Hutchison [1976] to use the relationship for crack tip stresses under contained plasticity, i.e. to use [Hutchinson, 1968; Rice & Rosengren, 1968]

$$\sigma_{xx} = \sigma_o\left(\frac{J_{pl}}{r\sigma_o\varepsilon_o}\right)^{\frac{1}{1+n}}\tilde{\sigma}_{xx}\left(\theta,\frac{1}{n}\right) \tag{2.2.46}$$

and similar equations for σ_{yy}, σ_{xy}, etc., to relate the crack tip parameters uniquely to the remotely applied load. Note that J_{pl} term in Equation 2.2.46 acts as a (plastic) stress field magnification factor similar to that of the stress-intensity factor in the elastic case. The form of the relationship that Shih and Hutchinson postulated is given by

$$\frac{J_{pl}}{\sigma_o\varepsilon_o a_o} = \left(\frac{\sigma}{\sigma_o}\right)^{n+1}\cdot\hat{J}\left(\frac{a}{b},n\right) \tag{2.2.47}$$

where $\hat{J}$ is a function only of relative width (a/b) and *n*. An alternate form of Equation 2.2.47 that has been previously used in computer codes [Kumar, et al., 1980; Kumar, et al., 1981; Weerasooriya & Gallagher, 1981] is

$$J_{pl} = \alpha\sigma_o\varepsilon_o a \cdot f_1\left(\frac{a}{b}\right) \cdot h_1\left(\frac{a}{b}, n\right) \cdot \left(\frac{P}{P^T_o}\right)^{n+1} \qquad (2.2.48)$$

where P is the applied load (per unit thickness), P^T_o is the theoretical limit load (per unit thickness), f_1 is a function only of geometry and crack length, while h_1 depends on geometry, crack length, and the strain hardening exponent n. Shih and coworkers [Kumar, et al., 1980; Kumar, et al., 1981] have tabulated the functions for a number of geometries for conditions of plant stress and plane strain. From the reference tabulated data [also see Weerasooriya & Gallagher, 1981], these functions can be obtained by interpolation for any value within the *a/b* and *n* limits given; thus, the plastic (strain hardening) component of Equation 1.3.44 can be computed for any given applied load P from Equation 2.2.48.

EXAMPLE 2.2.1 *J* Estimated for Center Crack Panel

Figure 2.2.10 describes the geometry for this example wherein the width W is set equal to $2b$ and the load P is expressed per unit thickness. Using Equation 2.2.44 to describe the relationship between the elastic and plastic components, we have

$$J = \frac{K^2}{E'} + J_{pl}$$

From elastic analysis, the stress-intensity factor is known to be (see section 11):

$$K = \left(\frac{P}{2b}\right)\sqrt{\pi a \sec\left(\frac{\pi a}{2b}\right)}$$

For the strain hardening analysis, Equation 2.2.48 is employed, i.e., we use

$$J_{pl} = \alpha\sigma_o\varepsilon_o a \cdot f_1\left(\frac{a}{b}\right) \cdot h_1\left(\frac{a}{b}, n\right) \cdot \left(\frac{P}{P_o^T}\right)^{n+1}$$

For a center crack panel, the function f_1 is given by [Kumar, et al., 1980; Kumar, et al., 1981]

$$f_1\left(\frac{a}{b}\right) = \frac{2b - 2a}{2b}$$

and the limit load (per unit thickness) is given by either

$$P_o^T = \frac{4}{\sqrt{3}}\sigma_o(b - a)$$

for plane strain or by

$$P_o^T = 2\sigma(b - a)$$

for plane stress. The supporting data for calculating the function h_1 is supplied by the following tables for plane strain conditions and plane stress conditions. The other functions (h_2 and h_3) contained in these tables support displacement calculations. As indicated above, data are available for estimating the *J*-integral according to this approach for a number of additional (simple geometries). See Kumar, et al. [1981] and Weerasooriya & Gallagher [1981] for further examples.

Table of Values of h_1, h_2, and h_3 for the Plane Strain CCP in Tension
[Shih, 1979; Kumar, et al., 1980; Weerasooriya & Gallagher, 1981]

a/b		n = 1	n = 2	n = 3	n = 5	n = 7	n = 10	n = 13	n = 16	n = 20
1/4	h_1	2.535	3.009	3.212	3.289	3.181	2.915	2.625	2.340	2.028
	h_2	2.680	2.989	3.014	2.847	2.610	2.618	1.971	1.712	1.450
	h_3	0.536	0.911	1.217	1.639	1.844	1.554	1.802	1.637	1.426
3/8	h_1	2.344	2.616	2.648	2.507	2.281	1.969	1.709	1.457	1.193
	h_2	2.347	2.391	2.230	1.876	1.580	1.276	1.065	0.890	0.715
	h_3	0.699	1.059	1.275	1.440	1.396	1.227	1.050	0.888	0.719
1/2	h_1	2.206	2.291	2.204	1.968	1.759	1.522	1.323	1.155	0.978
	h_2	2.028	1.856	1.600	1.230	1.002	0.799	0.664	0.564	0.466
	h_3	0.803	1.067	1.155	1.101	0.968	0.796	0.665	0.565	0.469
5/8	h_1	2.115	1.960	1.763	1.616	1.169	0.863	0.628	0.458	0.300
	h_2	1.705	1.322	1.035	0.696	0.524	0.358	0.250	0.178	0.114
	h_3	0.844	0.937	0.879	0.691	0.522	0.361	0.251	0.178	0.115
3/4	h_1	2.072	1.732	1.471	1.108	0.895	0.642	0.461	0.337	0.216
	h_2	1.345	0.857	0.596	0.361	0.254	0.167	0.114	0.081	0.051
	h_3	0.805	0.700	0.555	0.359	0.254	0.168	0.114	0.081	0.052

Table of Values of h_1, h_2, and h_3 for the Plane Stress CCP in Tension
[Shih, 1979; Kumar, et al., 1980; Weerasooriya & Gallagher, 1981]

a/b		n = 1	n = 2	n = 3	n = 5	n = 7	n = 10	n = 13	n = 16	n = 20
1/4	h_1	2.544	2.972	3.140	3.195	3.106	2.896	2.647	2.467	2.196
	h_2	3.116	3.286	3.304	3.151	2.926	2.595	2.288	2.081	1.814
	h_3	0.611	1.010	1.352	1.830	2.083	2.191	2.122	2.009	1.792
3/8	h_1	2.344	2.533	2.515	2.346	2.173	1.953	1.766	1.608	1.431
	h_2	2.710	2.621	2.414	2.032	1.753	1.473	1.279	1.134	0.988
	h_3	0.807	1.195	1.427	1.594	1.570	1.425	1.267	1.133	0.994
1/2	h_1	2.206	2.195	2.057	1.809	1.632	1.433	1.300	1.174	1.000
	h_2	2.342	2.014	1.703	1.299	1.071	0.871	0.757	0.666	0.557
	h_3	0.927	1.186	1.256	1.178	1.040	0.867	0.758	0.668	0.560
5/8	h_1	2.115	1.912	1.690	1.407	1.221	1.012	0.853	0.712	0.573
	h_2	1.968	1.458	1.126	0.785	0.617	0.474	0.383	0.313	0.256
	h_3	0.975	1.053	0.970	0.763	0.620	0.478	0.386	0.318	0.273
3/4	h_1	2.073	1.708	1.458	1.208	1.082	0.956	0.745	0.646	0.532
	h_2	1.611	0.970	0.685	0.452	0.361	0.292	0.216	0.183	0.148
	h_3	0.933	0.802	0.642	0.450	0.361	0.292	0.216	0.183	0.149

In the application of Equation 2.2.44 to structural material problems, it has been found [Bucci, et al., 1972] that better correlation with experimental results is obtained if one uses the plasticity enhanced, effective crack length (a_e) in plane of the physical crack length (a) in the elastic component expressions. The effective crack length utilized by Bucci, et al. [1972] was based on the Irwin plastic zone size correction, i.e. the effective crack length was given by

$$a_e = a + r_y \tag{2.2.52}$$

where

$$r_y = \frac{1}{x\pi}\left(\frac{K}{\sigma_o}\right)^2 \tag{2.2.53}$$

with $x = 2$ for plane stress and $x = 6$ for plane strain. K represents the stress-intensity factor.

2.2.6.3 Crack Opening Displacement

The crack opening displacement (COD) parameter was proposed to provide a more physical explanation for crack extension processes. [Wells, 1961; Burdekin & Stone, 1966] The philosophy was based on a crack tip strain based model of cracking that would allow for the occurrence of elastic-plastic material behavior. The initial modeling, however, was based on elasticity solutions of crack tip displacements. Equation 2.2.54 describes the x and y displacements (u and v, respectively) in the crack tip region of an elastic material:

$$u = \frac{K}{2G}\left(\frac{r}{2\pi}\right)^{1/2} cos\frac{\theta}{2}\left[\kappa - 1 + 2sin^2\frac{\theta}{2}\right] \tag{2.2.54a}$$

$$v = \frac{K}{2G}\left(\frac{r}{2\pi}\right)^{1/2} sin\frac{\theta}{2}\left[\kappa + 1 - 2cos^2\frac{\theta}{2}\right] \tag{2.2.54b}$$

where $\kappa = 3 - 4\nu$ for plane strain and $\kappa = (3 - \nu)/(1 + \nu)$ for plane stress, and where G is the shear modulus ($G = 0.5E/(1 + \nu)$). If the angle θ is chosen to be 180° (π), the displacements are those associated with crack sliding (u component) or opening (v component). Under mode 1 (symmetrical) loading, the case covered by Equation 1.3.54, the sliding displacement term is noted to be identically zero; and all displacement is perpendicular to the crack, i.e. only opening is observed. Based on Equations 2.2.54 and 2.2.18 and the definition of shear modulus (G), the displacement of the crack relative to its longitudinal axis (x axis) is

$$v = 4\frac{K}{E'}\left(\frac{r}{2\pi}\right)^{1/2} \tag{2.2.55}$$

The relative movement of the crack faces is the COD and it is twice the value obtained by Equation 2.2.55, i.e.

$$COD = 2v \tag{2.2.56}$$

One immediate observation is that COD will vary as a function of position along the crack, and that the COD at the crack tip, i.e. at $r = 0$, is zero. In the quasi-elastic-plastic analysis performed by Wells, the crack was allowed to extend to an effective length (a_e), one plastic zone radius larger than the physical crack length (a); the crack opening displacement was then determined at

the location of the physical crack tip. Figure 2.2.15 describes the model used to define the crack tip opening displacement (CTOD). The Wells modeling approach leads one to

$$CTOD = 8\frac{K}{E'}\left(\frac{r_y}{2\pi}\right)^{1/2} \tag{2.2.57}$$

which after some simplification gives the CTOD as

$$CTOD = \frac{4}{\pi}\frac{K^2}{E'\sigma_o} \tag{2.2.58}$$

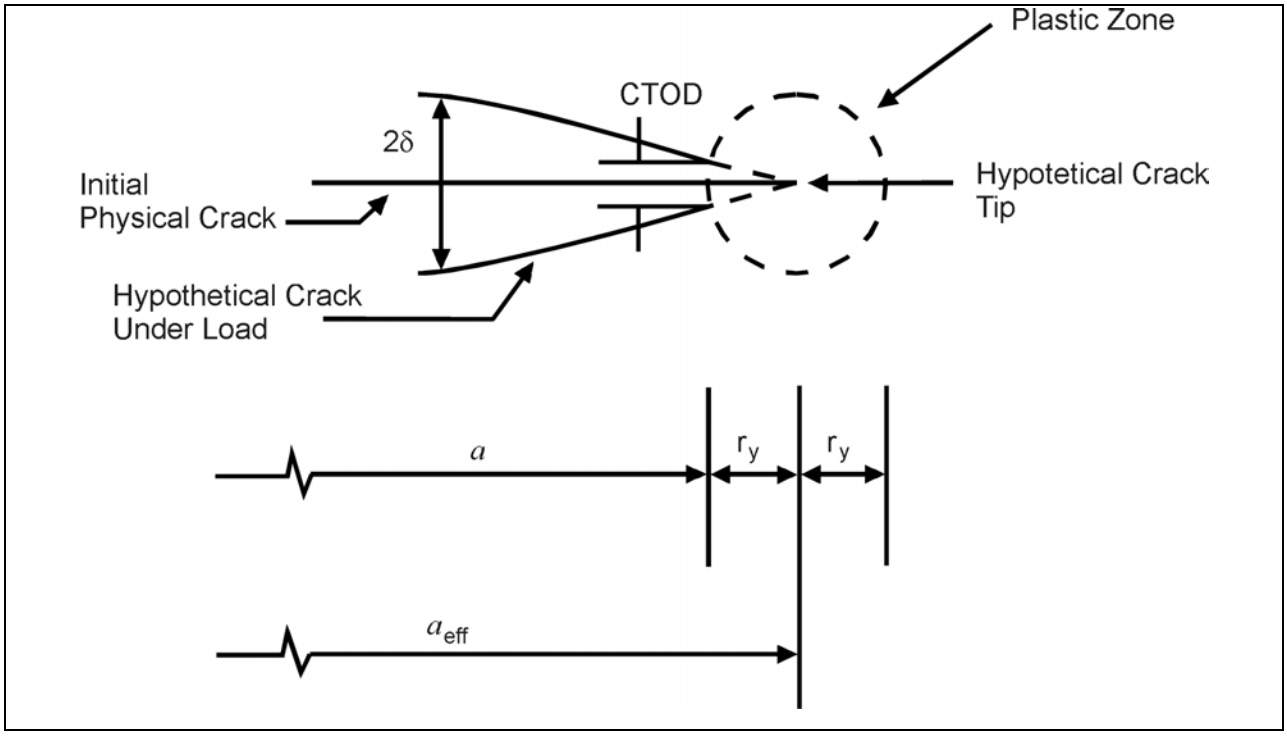

Figure 2.2.15. Description of Model Used to Establish the CTOD Under Elastic Conditions

It is immediately seen that the CTOD is directly related to the stress-intensity factor for elastic materials; thus, for elastic materials, fracture criteria based on CTOD are as viable as those based on the stress-intensity factor parameter. The other relationships developed between *K* and *G* or *J* in this section allow one to directly relate *G* and *J* to the CTOD in the elastic case.

In the late 1960's, Dugdale [1960] conducted an elasticity analysis of a crack problem in which a zone of yielding was postulated to occur in a strip directly ahead of the crack tip. The material in the strip was assumed to behave in a perfect plastic manner. The extent of yielding was determined such that the singularity at the imaginary crack tip (see Figure 2.2.16) was canceled due to the balancing of the remote positive stress-intensity factor with the local yielding negative stress-intensity factor. The Dugdale quasi-elastic-plastic analysis provided an estimate of the

relative displacement of the crack surfaces for a center crack (crack length = $2a$) in an infinite plate subjected to a remote tensile stress (σ) and having a yield strength equal to σ_o, the CTOD is

$$CTOD = \frac{8a\sigma_o}{\pi E'} \ell n\left(sec\left(\frac{\pi\sigma}{2\sigma_o} \right) \right) \tag{2.2.59}$$

at the tip of the physical crack tip (a) and the extent of the plasticity ahead of the crack is

$$\omega = a\left[sec\left(\frac{\pi\sigma}{2\sigma_o} \right) - 1 \right] \tag{2.2.60}$$

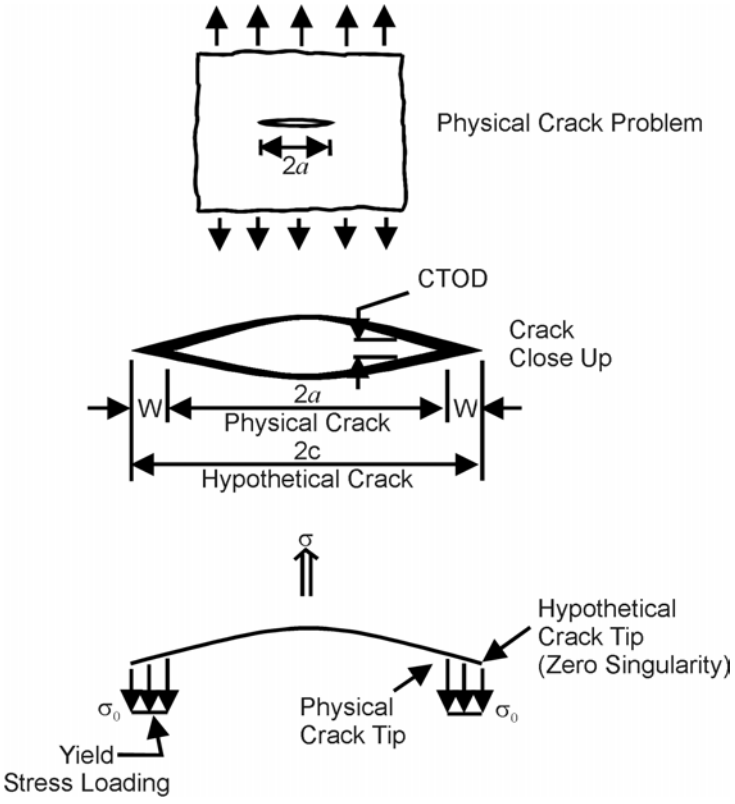

Figure 2.2.16. Dugdale Type Strip Yield Zone Analysis

For the case of small scale yielding, i.e., when $\frac{\sigma}{\sigma_o}$ is low, the CTOD and extent of plasticity (ω) reduce to

$$CTOD \cong \frac{\sigma^2 \pi a}{E'\sigma_o} = \frac{K^2}{E'\sigma_o} \tag{2.2.61}$$

and

$$\omega \cong \frac{\pi}{8}\frac{K^2}{\sigma_o 2} \qquad (2.2.62)$$

It can first be noted that the extent of the plasticity (ω) is only about 20% higher than would be predicted using the Irwin estimate of the plastic zone diameter ($2r_y$). The level of CTOD estimated by Equation 2.2.61 also compares favorably with that given by Equation 2.2.58; Equation 2.2.61 gives an estimate that is about 30 percent lower than Equation 2.2.58. Numerous other studies have shown that the CTOD is related to the stress-intensity factor under conditions of small scale yielding through

$$CTOD = \alpha \frac{K^2}{E'\sigma_o} \qquad (2.2.63)$$

where the constant α ranges from about 1 to 1.5. Experimental measurements [Bowles, 1970; Roberson & Tetelman, 1973] have indicated that α is close to 1.0, although there is substantial disagreement about the location where CTOD should be measured.

One difficulty with elastic analyses is that the crack actually remains stationary and thus one must reposition the crack through a quasi-static crack extension so that the CTOD for the actual crack can be assessed. During loading, cracks in ductile materials tend to extend through a slow tearing mode of cracking prior to reaching the fracture load level. In these cases, the amount of opening that occurs at the initial crack tip represents one measure of the crack tip strain; but, this parameter depends not only on load, initial crack length and material properties, it also depends on the amount of crack extension from the initial crack tip. Rice and co-workers [Rice, 1968b; Rice & Tracey, 1973] attempted to provide an alternate choice of locating the position where CTOD would be measured. They found that when the CTOD was determined for the position shown in Figure 2.2.17, the CTOD and J integral were related (for ideally plastic materials) by

$$CTOD = d_n \frac{J}{\sigma_o} \qquad (2.2.64)$$

For the case of plane stress behavior, d_n is unity and for plane strain behavior, d_n is about 0.78.

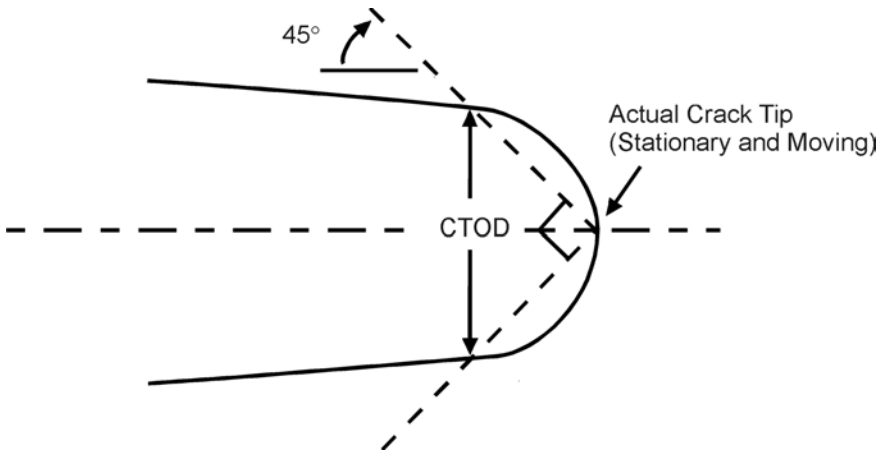

Figure 2.2.17. Definition of the Crack Tip Opening Displacement (CTOD)

For strain hardening materials controlled by Equation 2.2.45, Shih and co-workers [Shih & Kumar, 1979; Shih, 1979] have shown that Equation 2.2.64 relates J and CTOD if the constant d_n is replaced with a function that is strongly dependent on the strain hardening exponent and mildly dependent on the ratio σ_o/E. Thus, there is a direct relationship between CTOD and J throughout the region of applicability of the J-Integral and CTOD can likewise be considered a measure of the magnitude of the crack tip stress-strain field.